

Supplementary Information

An Open-source Model for Simulation and Corrective Measure Assessment of the 2021 Texas Power Outage

Dongqi Wu^{1,†}, Xiangtian Zheng^{1,†}, Yixing Xu², Daniel Olsen², Bainan Xia², Chanan Singh¹, and Le Xie^{1,3,*}

¹Department of Electrical and Computer Engineering, Texas A&M University, College Station, Texas, USA

²Breakthrough Energy Sciences, Seattle, Washington, USA

³Texas A&M Energy Institute, College Station, Texas, USA

*Corresponding author: le.xie@tamu.edu

†Co-first author

Supplementary Notes:

- Supplementary Note 1: Remarks on the gap between actual and estimated generation capacity
- Supplementary Note 2: Remarks on the mismatch between actual and simulated load shedding
- Supplementary Note 3: Remarks on the benchmark of load shedding allocation
- Supplementary Note 4: Relation between natural gas generation derate and gas supply scarcity
- Supplementary Note 5: Incorporate gas supply scarcity into natural gas thermal generation winterization
- Supplementary Note 6: Remarks on the performance of HVDC and demand response
- Supplementary Note 7: Remarks on the performance of winterization of various sources in multiple regions

Supplementary Methods:

- Supplementary Method 1: Transmission line upgrade around the interconnection nodes of the HVDC lines

Supplementary Table:

- Supplementary Table 1: Selective generation units winterization in portfolio 1, 2 and 3

Supplementary Figures:

- Supplementary Figure 1: Actual and counterfactual wind and solar generation
- Supplementary Figure 2: Conceptual figure of four measures

Supplementary Notes

Supplementary Note 1: Remarks on the gap between actual online and estimated generation capacity

There are two periods that have apparent gap between actual and estimated generation capacity as shown in Fig. 1. The first period is before 12 a.m. February 15, when the EEA 3 has not been launched. The reason for this mismatch is that the estimated generation capacity includes all non-outaged generation that is not necessarily online, and it is normal that generation units are offline according to the dispatch or scheduled seasonal maintenance. Therefore, the estimated generation capacity is higher than the actual online generation capacity. The second period is after 12 p.m. February 16, when the gap becomes increasingly large. We suspect it could involve several causes, of which the main one may be attributed to the generators whose de-rating and outage are not disclosed in the public report¹. Besides, the good match between 12 a.m. February 15 and 12 p.m. February 16 is because all available generation must be required online under such emergency conditions. Since we focus on the blackout event period, it is reasonable to use the estimated generation capacity instead of the actual online capacity to achieve the most accurate granularity.

Supplementary Note 2: Remarks on the mismatch between actual and simulated load shedding

Here we separate the period from February 15 to February 18 into three parts, namely the load shedding rising stage from 0 a.m. to 8 p.m. February 15, the load shedding stable stage from 8 a.m. February 15 to 12 p.m. February 16 and the load restoration stage from 1 p.m. February 16 to 12 a.m. February 18. During the load shedding rising stage, actual and simulated ENS are respectively 277,625 MWh and 274,316 MWh, of which the relative error is -1.19%. During the load shedding stable stage, actual and simulated ENS are respectively 292,778 MWh and 331,210 MWh, of which the relative error is 13.12%. During the load restoration stage, actual and simulated ENS are respectively 428,388 MWh and 324,115 MWh, of which the relative error is -24.34%. The mismatch between actual and simulated total ENS is mainly derived from the later two stages. The gap during the load shedding stable stage is mostly due to multiple factors such as system topology, system congestion pattern and load shedding strategy (shown in Methods). However, to our best ability, this is the closest result we can obtain based on only publicly available materials, in which limitations include the low geographical resolution of generation, demand and outage data as well as lack of detailed load shedding protocols or event logs in ERCOT internal documentations. The significant mismatch during the load restoration stage shows that the actual load restoration is slower than the simulated one, which may reasonably attribute to the requirements by system transient stability, unknown load regulation, and unreported technical load restoration issues that nevertheless are beyond this paper's scope and need more attention for future research.

Supplementary Note 3: Remarks on the benchmark of load shedding allocation

Although we have acquired county-level outage data from PowerOutage.com² that show the number of customers with and without electricity during the Texas windstorm event, those data are not appropriate for simulation purposes as they do not provide actual online and offline capacity (in kW/MW). In our simulation, the loads are allocated and scaled based on their rated MW capacity and total ERCOT historical hourly load in each weather zone. While it would be intuitive to draw a direct relationship between the number of disconnected customer and the total capacity of those customers, we unfortunately do not have the necessary data with high enough resolution to do so as the load data in our synthetic network is aggregated and represents the total capacity of entire towns which include residential, commercial and industrial load altogether.

Supplementary Note 4: Relationship between natural gas generation derating and gas supply scarcity

Our hypothesis is that all natural gas generation derating is derived from the gas supply scarcity and the remaining full outage is derived from equipment failures at power plants. The ERCOT blackout event review³ includes some information related to the generation outages, which documented that the cumulative generation capacity forced out throughout the event is 46,249 MW, cumulative number of generators outage throughout the event is 356 and cumulative gas generation de-rated due to supply issues is 9,323 MW. Here the "cumulative capacity" includes all units that have failed at some point, regardless of whether it comes back later during the event, as defined as in the 2011 ERCOT winter event report⁴. To verify the hypothesis, we calculate the cumulative generation capacity forced out and cumulative number of generators outage based on the generation outage report¹, which are respectively 47,946 MW and 316. The relative error between estimated and reported values are 3.67% and 11.23%, which validates the correctness of the calculate method. The mismatch between real and reported cumulative number of generator outages is in line with our expectation because about 10% of generation plants deny to release of the outage information to the public¹. In the same way, we calculate the cumulative generation derating that equals to 10,608 MW, which has 13.78% relative error compared to the reported 9,323 MW. To simplify the problem, we confirm that the proposed hypothesis roughly matches the reality which indicates that all natural gas generation derating are cause by gas supply scarcity.

Supplementary Note 5: Incorporating gas supply scarcity into natural gas thermal generation winterization

As shown in Supplementary Note 4, we are able to roughly separate the outage/de-rating of generators that are caused by lack of gas supply and those that are caused by un-winterized power plant facilities. With this information, we are able to incorporate gas supply interruption in our counterfactual simulations that involve the hypothetical weatherization of natural gas generators. We only apply weatherization treatments to generators that are completely out-of-service as shown in the ERCOT unit outage data. For each of those generators, we calculate the amount of de-rating of other in-service but de-rated generators in the same county by assuming that the availability of gas supply is roughly the same across gas generators in the same county. Hence, even when those completely out generators are in service as a result of weatherization, they still cannot run at their maximum capacity due to the lack of gas supply. In counterfactual simulation, the de-rating caused by gas supply is done by giving additional natural gas generators a de-rating multiplier that is determined by the level of de-rating of its neighbouring generators in the same county.

Supplementary Note 6: Remarks on the performance of HVDC and demand response

In Fig. 4b and 4c, the effect of HVDC and demand response on forced load shedding is different even for the same total capacity. This difference is mainly caused by the difference in modelling these two types of corrective measures. For the modelling of additional HVDC, we have added two converter stations into the synthetic network: one in the city of Roscoe in the West zone representing a DC tie to California, one in the city of Bryan in the Coast zone representing a DC tie to Florida. Transmitting power from these two converter station to the rest of the grid is limited by network congestion, which can result in remote loads not getting power from HVDC interconnections and thus they must be shed even when there is available power supply from the HVDC ties. In contrast, for the modelling of demand response, we assume the additional load-capacity is split across the entire network, which is less likely to cause congestion than concentrated high-capacity energy supply like the HVDC converter stations. Moreover, since the system demand is still reduced after introducing demand response (but on a voluntary basis), the lower demand also alleviates the congestion pattern in the network which leads to more effective energy use.

Supplementary Note 7: Remarks on the performance of winterization of various sources in multiple regions

Table 1 in the main text has shown that for the same amount of MW of weatherization, the difference in effectiveness of different fuel types can be very different. This difference is mainly caused by the severity of outage and derating during the event across generator types. Some type of generators, such as natural gas, are more vulnerable to cold weather than others and have suffered much higher levels of outage and derating, thus weatherization treatment would be more effective. In contrast, coal and nuclear generators are much less affected by the winter storm (probably due to their larger size), thus additional weatherization treatment won't improve the situation much. In short, the more severe a generator is affected, the more effective will its weatherization be. Moreover, even with complete weatherization, the actual capacity of wind turbines is affected by the wind strength. For example, the wind strength between 9 a.m. February 15 and 8 p.m. February 16 is weak, hence during this time period wind turbines cannot provide much power even if they are fully weatherized.

Supplementary Methods

Supplementary Method 1: Transmission line upgrade around the interconnection nodes of the HVDC lines

In our counterfactual case studies we have added two additional HVDC converter stations that represent ties to California and Florida to the original synthetic grid network. Each station is capable of transmitting at a maximum 2000 MW of real power into the ERCOT network. This additional power injection will significantly overload the AC transmission grids near the point of common coupling as their specifications are not designed to handle the additional power flow. To accommodate the new resources, we have up-scaled the thermal limit of AC transmission lines in the neighbouring region to avoid line overflowing. We have designed a iterative algorithm to upgrade the AC transmission line appropriately without disrupting the congestion pattern in the original network.

We first model the topology of a transmission network as an un-directed graph, where each bus is represented as a vertex and each branch is represented as an edge. Let B denote the set of all buses (vertices) in the graph; let $L = L_{ij} \forall i, j \in B$ denote the set of all branches (edges). The *distance* between two vertices i and j is denoted as D_{ij} . The real power flow in a line L_{ij} is P_{ij} . For each transmission there exists a thermal rating, P^{max} , that dictates the maximum allowed power flow along the line. The thermal limit is used in OPF formulation to ensure that the power flow of all lines in the network is lower than the thermal limit, $P_{ij} <= P_{ij}^{max} \forall i, j \in B$. We define the line Load Factor $\rho_{ij} = P_{ij}/P_{ij}^{max}$ as the ratio between the line flow to its thermal limit. With the addition of a new power source such as an HVDC converter, the line flow pattern across the network will change to reflect the new power flow solution. Most likely, the power flow in the lines that are close to the converter station will increase drastically as the capacity of HVDC lines is usually much larger than the power absorption of local loads in the region and will cause lines to overflow. To upgrade those lines appropriately, we take an iterative approach to ensure that the load factor ρ of lines in nearby regions remain unchanged before and after adding the new HVDC tie with a designated max capacity. The detailed algorithm is presented as follow:

Algorithm 1: AC Transmission Network Upgrade for Additional HVDC Links

```

Define the maximum capacity of new HVDC tie  $P_{dc}$  and increment stepsize  $\Delta P_{dc}$ 
Define the maximum distance  $N$  within which the lines will be upgraded
Select a heavily loaded profile snapshot as baseline
Select a bus  $o \in B$  in the network as the location for new DC converter station
Find the sets of buses  $[B^1, B^2, \dots, B^N]$  such that  $D_{oj} == n, \forall j \in B^n$  through recursive graph tracing
Find the sets of all lines  $[L^1, L^2, \dots, L^N]$  that connects the buses of neighbouring distance:  $L^n = \{L_{ij} | i \in B^{n-1}, j \in B^n\}$ 
Run DCOPF to determine initial line flows  $P_{ij}^{base} \forall i, j \in B$ 
Calculate load factor for lines that require upgrading,  $\rho_{ij}^{base} \forall i, j \in [L^1, L^2, \dots, L^N]$ 
Initialize the capacity of new DC tie,  $P^{dc} = \Delta P_{dc}$ 
while  $P^{dc} < P_{max}^{dc}$  do
    Set the power injection at bus  $o$ ,  $P_o = P_{dc}$ 
    Solve DCOPF to obtain new line flows with additional HVDC injection  $P_{ij} \forall i, j \in B$ 
    for  $n = [1, 2, \dots, N]$  do
        Upgrade thermal rating of lines  $P_{ij}^{max} = \max(P_{ij}/\rho_{ij}^{base}, P_{ij}^{max}) \forall i, j \in L^n$ 
    end for
    Increment  $P_{dc} = P_{dc} + \Delta P_{dc}$  iteratively to ensure convergence
end while

```

Supplementary Table

Supplementary Table 1: Selective generation units winterization in portfolio 1, 2 and 3

Table 1. Allocation of Winterized Capacity (MW) in Portfolio 1

Weather Zone	Far West	West	North	East	Coast	North Central	South Central	South
Natural Gas	2000	0	0	0	2000	2000	0	2000
Coal	0	0	0	0	1000	0	0	0
Wind	0	0	0	0	0	0	0	0
Nuclear	0	0	0	0	0	0	1000	0

Table 2. Allocation of Winterized Capacity (MW) in Portfolio 2

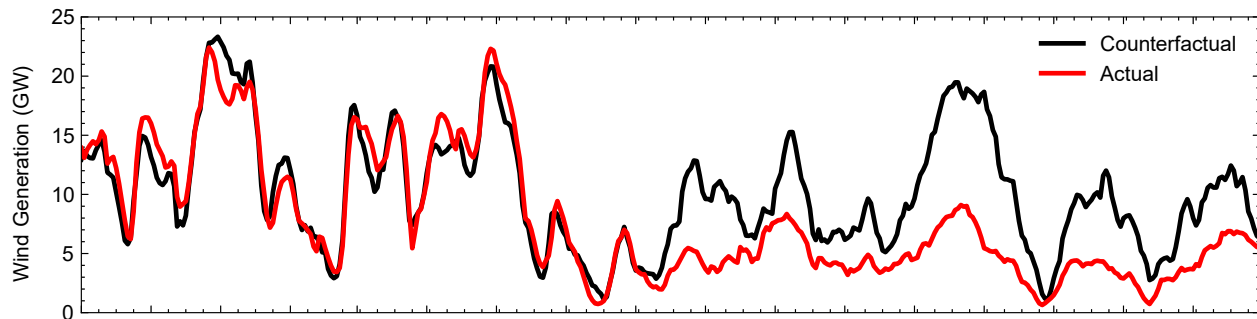
Weather Zone	Far West	West	North	East	Coast	North Central	South Central	South
Natural Gas	3500	500	1000	1000	2500	3000	1000	2500
Coal	0	0	0	0	1000	0	0	500
Wind	500	1000	500	500	0	0	0	0
Nuclear	0	0	0	0	0	0	1000	0

Table 3. Allocation of Winterized Capacity (MW) in Portfolio 3

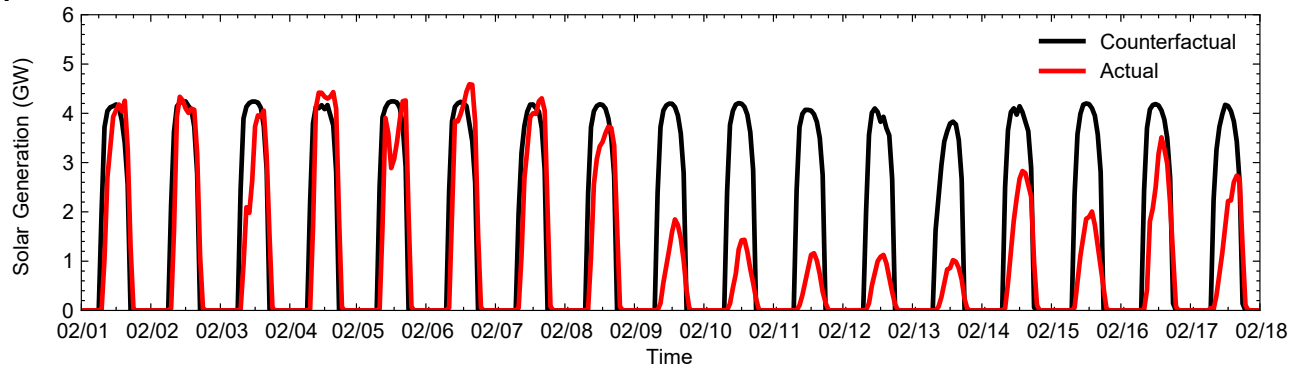
Weather Zone	Far West	West	North	East	Coast	North Central	South Central	South
Natural Gas	3500	500	1000	1000	2500	3000	1000	2500
Coal	0	0	0	0	1000	0	0	500
Wind	500	1000	500	500	0	0	0	0
Nuclear	0	0	0	0	0	0	1000	0

Supplementary Figures

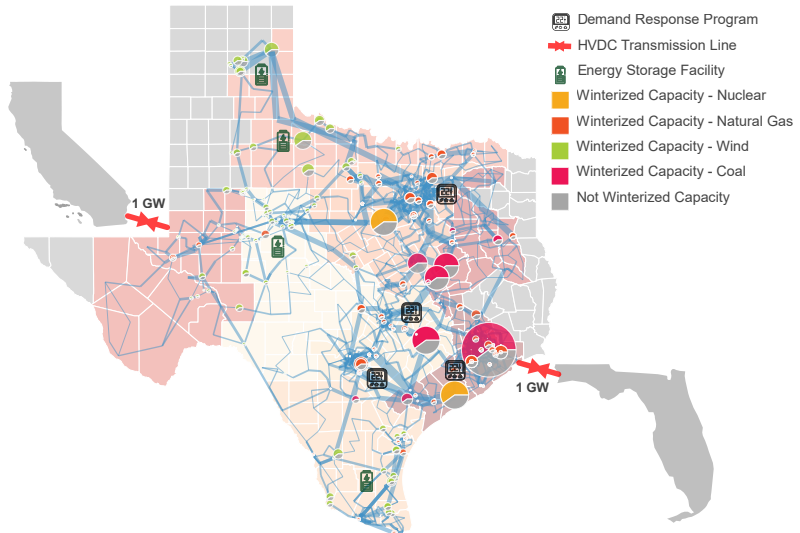
a.



b.



Supplementary Figure 1. Actual and counterfactual wind and solar generation. Note that the counterfactual wind generation is estimated based on the weather data⁵ as described in the literature⁶, while the counterfactual solar generation is obtained from ERCOT solar forecast data⁷. The model-based renewable generation estimation is preferred because of its higher granularity. However, for the case of counterfactual solar generation, the lack of relevant weather data prevents this model-based method and instead we have to use the ERCOT solar forecast data.



Supplementary Figure 2. Conceptual diagram of geographical distribution of four corrective measures in simulation. It illustrate a combination of 60% facility winterization, 2 GW HVDC lines, 2 GW up-scaled demand response program and 4 GWh strategic energy storage facility. Here the generators of thermal and renewable energy evenly implement 60% winterization. The two long-distance HVDC lines with total 2 GW deliver the power from California through the Western Interconnection to the West zone and from Florida through the Eastern Interconnection to the Coast zone. The up-scaled demand response program is mainly deployed in four metropolises. The energy storage facilities are deployed around the location with rich renewable generation.

References

1. The Electric Reliability Council of Texas. Generation resource and energy storage resource outages and derates, feb 10-19, 2021 (Available: http://www.ercot.com/content/wcm/lists/226521/Unit_Outage_Data_20210312.pdf [Online], 2021).
2. Bluefire Studios LLC. Poweroutage.us products (Available: <https://poweroutage.us/products> [Online], 2021).
3. B. Magness. Review of february 2021 extreme cold weather event – ercot presentation (Available: <https://apnews.com/article/houston-hypothermia-weather-conroe-texas-8323ab5f5c1612e632f7f2e6c2c20358> [Online], 2021).
4. Federal Energy Regulatory Commission and North American Electric Reliability Corporation. Report on outages and curtailments during the southwest cold weather event of february 1-5, 2011 (Available: <https://www.ferc.gov/sites/default/files/2020-04/08-16-11-report.pdf> [Online], 2011).
5. National Oceanic and Atmospheric Administration. Rapid refresh (rap) (Available: <https://www.ncdc.noaa.gov/data-access/model-data/model-datasets/rapid-refresh-rap> [Online], 2021).
6. Xu, Y. *et al.* Us test system with high spatial and temporal resolution for renewable integration studies. In *2020 IEEE Power & Energy Society General Meeting (PESGM)*, 1–5 (IEEE, 2020).
7. The Electric Reliability Council of Texas. Grid information (Available: <http://www.ercot.com/gridinfo> [Online], 2021).